Foam Electrospinning: A Multiple Jet, Needle-less Process for Nanofiber Production

Alina K. Higham, Christina Tang, Alexandra M. Landry, Monty C. Pridgeon, Esther M. Lee, Anthony L. Andrady, and Saad A. Khan

Dept. of Chemical and Biomolecular Engineering, North Carolina State University, 911 Partners Way, Raleigh, NC 27695

DOI 10.1002/aic.14381

Published online February 19, 2014 in Wiley Online Library (wileyonlinelibrary.com)

A multiple jet, needle-less process to fabricate electrospun nanofibers from foamed columns, produced by injecting compressed gas through a porous surface into polymer solutions, capable of circumventing syringe electrospinning shortcomings such as needle clogging and restrictions in production rate is presented. Using polyvinyl alcohol and polyethylene oxide (PEO) as model systems, we identify key design, processing, and solution parameters for producing uniform fibers. Increasing electrode surface area produces thicker mats, suggesting charge distribution through the bulk foam facilitates electrospinning. Similar trends between foam and syringe electrospinning are observed for collection distance, electric field strength, and polymer concentration. Interestingly, the empirical correlation between polymer entanglement and fiber formation are found to be similar for both foam and traditional needle electrospinning, but the fiber crystallinity shows enhancement with foam electrospinning. In addition, foam electrospinning with a PEO-nonionic surfactant system yields two orders of magnitude increase in production rate compared to syringe electrospinning.
 AIChE J, 60: 1355–1364, 2014

Keywords: nanotechnology, nanofiber, electrospinning

Introduction

Nanofibers, fibers with average diameters ranging from about 50 nm to less than a micron, are currently used in several applications such as catalysis, tissue scaffolding, protective clothing, drug delivery, and gas sensors and so forth, due to their high aspect ratios.[1–7] These nanofibers are traditionally fabricated via a simple technique called electrospinning,[8–11] where an electric field is applied to a droplet, deforming it into a conical shape, known as a Taylor cone.[12] Once the induced charges overcome the solution surface tension, a jet ejects from the apex of the cone toward a grounded collection plate, where whipping and solvent evaporation reduce the jet diameter and the resulting fiber is deposited as a nonwoven mat.[13,14]

Although simple, syringe-based approaches may experience needle clogging, which occurs when dried polymer remains on the spinneret tip when solvent evaporates before the solution can be electrospun, preventing fiber production. Additionally, low polymer concentration solutions and low flow rates, typically below 1 mL/h are used, limiting fiber production rates. Multiple needles cannot be placed at high spatial density to improve the rate of nanofiber production due to strong charge repulsion between the jets.[15–20] Developing techniques capable of improving process throughput and preventing needle clogging has been an area of recent interest.

Recently, electrospinning polymer nanofibers from bubbles has been demonstrated using a single-nozzle apparatus,[21–24] and empirical relationships were reported correlating fibers to select process parameters, such as electric field strength[25] and solution concentration.[26–28] However, these studies were limited to single bubble or submerged nozzle setups operating at gas pressures less than 0.5 psi.[25] Additionally, electrospinning from a single bubble in a polymer bath leads to the possibility of fibers initiating from locations other than the bubble surface, such as the container edge and solution surface. A comparison of electrospun fibers from novel approaches to syringe electrospun fibers has yet to be established.

In this study, we examine a new approach of needle-less electrospinning utlitizing foams. Unlike previous work from single or a few bubbles produced from a single nozzle in a vast pool of liquid, we are working with a sample spanning high gas volume fraction foam, the characteristics of which are drastically different from individual/few bubbles in terms of structure, stability, formation, and dynamics. Critical questions we seek to answer include the following. Can we achieve electrospun nanofibers from a foamed surface wherein the films of the foam serve as the point of fiber emanation? Given that we are electrospinning from a film rather than a bulk liquid, does the regime of electrospinnability in terms of polymer chain entanglement change, and finally, are the final fiber properties affected because of the

Additional Supporting Information may be found in the online version of this article.

Correspondence concerning this article should be addressed to S. A. Khan at khan@eos.ncsu.edu.

new configuration? Our focus is to examine these issues and provide a first step toward a new methodology, while relegating a study of foam dynamics and its relevance, if any, to future studies.

Experimental Section

Materials

Polyvinyl alcohol (PVA) (average molecular weight 205,000 g/mol, 88% hydrolyzed), nonionic Triton X-100® surfactant, and Rhodamine B dye were used as received from Sigma Aldrich. Polyethylene oxide (PEO) was used as received from Polysciences (average molecular weight 600,000 g/mol).

Solution preparation and characterization

PVA was dissolved in deionized water between 1 and 9 wt % and stirred at 60°C until homogenous, while PEO was dissolved in deionized water between 1 and 7 wt % and stirred at room temperature overnight until homogenous. In some cases, Triton X-100® was dissolved along with PEO in deionized water. Zero-shear viscosity was measured at 25°C using a 40-mm diameter, 2° cone, and plate geometry (TA Instruments AR-G2 rheometer). Surface tension measurements were made using an Attension Sigma 703D Tensiometer, utilizing a platinum Wilhelmy plate attachment. Conductivity measurements were performed using a conductivity module of a Mettler Toledo SevenMulti pH/conductivity/ion meter. The conductivity cell used was an InLab(R)731conductivity probe. This probe contains an integrated temperature sensor that can detect the temperature of the test sample during the conductivity measurement. Measurements of the conductivity and surface tension of the various solutions were done in triplicate and are given in a table as part of the Supporting Information.

Electrospinning

Electrospun fibers were created by injecting compressed carbon dioxide (Airgas National Welders) at a constant flow rate of 310 cubic centimeters per minute (ccm) and pressure of 20 pounds per square inch (psi) into polymer solutions through a fritted funnel (Fisher Scientific, pore size 4–5.5 μm for fine and 40–60 μm for coarse) coupled with a power supply (Matsusada High Precision, model AU-60P*0.5). Foam electrospinning parameters varied between 15 and 50 kV for voltage and 6 to 30 cm for collection distance (measured as the distance between the top of the funnel and grounded plate). For comparison, a syringe electrospinning method using a syringe fitted with a stainess steel needle (0.508 mm inner diameter) operating at a flow rate of 0.5 mL/h, collection distance of 20 cm, and applied voltage of 10–22 kV were used. The Nanospider™ manufactured by Elmarco with all accessories supplied by the manufacturer was used as additional comparison (for photographs, see Supporting Information).

The production rate from the foam electrospinning process was measured by subtracting the weight of remaining solution after electrospinning for a set amount of time from a known initial weight of solution. Calculation assumes all consumed solution forms fibers.

Fiber characterization

Resulting fiber mats were coated with a ~10 nm layer of gold and imaged using a scanning electron microscope (SEM) (FEI XL30 field emission SEM). Fiber size distributions and average diameters were obtained from the measurements of 100 fibers using ImageJ analysis software. Electrospun fiber crystallinity was measured by heating samples from 25 to 95°C at a rate of 10°C/min in a nitrogen environment using differential scanning calorimetry (DSC) (TA Instruments Q2000 calorimeter) and x-ray diffraction (XRD) patterns (Philips X'Pert PRO MRD HR XRD System), acquired at room temperature with Cu Kα radiation.

Results and Discussion

Foam electrospinning

We produce polymeric foams by injecting compressed carbon dioxide through a porous plate into a polymer solution. High voltage charge is applied to the system by immersing a copper electrode coupled to a high voltage power supply into the polymer solution, Figure 1A. Bubbles form and rise to the surface, producing a column of foam. When an electric field is applied, several perturbations form on the foam surface, resulting in multiple polymer jets ejecting toward the collection plate directly above the foam, Figure 1B.

During the process, some bubbles deform into upward-directed, hollow conical shapes, Figure 1C, analogous to the Taylor cone in syringe electrospinning. This phenomenon has been previously reported by Varabhas, who found the angle of the Taylor cone-like perturbation on the bubble surface to be equal to that reported for syringe electrospinning.[29] Additionally, we have observed the formation of multiple perturbations on a single bubble, which has not been previously reported in single bubble studies. There does not appear to be a significant change in the height of the foam over the course of an experiment (typically 15 min). Movement of the electrospinning jet along the bubble surface helps to perpetuate the electrospinning process. Additionally, the influx of gas may cause some bubbles to grow beyond their maximum size and burst, presenting a discontinuity which may lead to fibers of finite length.[30]

As the electrospun jets initiate from the surface of a foam compared to a point source in syringe electrospinning, the geometry of the electrode and manner for charging the system must be considered for design of the process. The study includes a solution of 7 wt % PVA in water, as it is a model electrospinning system, and three electrode geometries: a ringed wire (one-dimensional [1-D], 0.25 in^2 surface area), a wire mesh (2-D, 1.9 in^2 surface area), and a wire "bird's nest" (3-D, 5.8 in^2 surface area), shown in Figure 2. Using the 1-D electrode, few jets eject from the foam surface, producing a sparse mat. Two- and three-dimensional electrodes produce thicker mats. We attribute the improved fiber yield to the increase in electrode surface area, the higher surface area allowing sufficient contact between liquid and the electrode to adequately charge the liquid and improve the distribution of electrical charges throughout the polymer solution and foam. As the 2- and 3-D electrodes produce similar fibers under comparable process parameters, the 2-D electrode was used in subsequent experiments due to simplicity.

Process parameters

Using 7 wt % PVA as a model system based on our previous work,[31] we explored the effect of various apparatus parameters including electric field strength and collection distance. The effects of electric field strength and collection

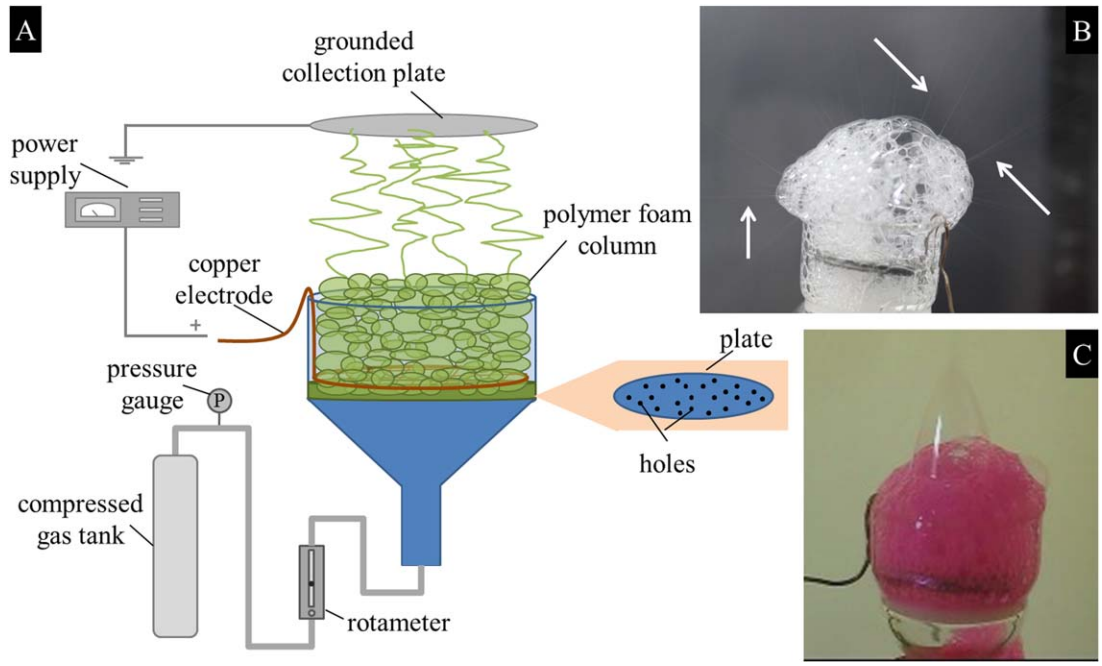

Figure 1. (A) A schematic of the foam electrospinning apparatus.

Digital photographs of the foamed column during experiments utilizing a compressed gas flow rate of 310 ccm at 20 psi showing, (B) multiple polymer fibers (some shown by arrows) forming when foam electrospinning 5 wt % PEO and 0.1 wt % Triton X-100® with 40 kV of applied voltage at a collection distance of 30 cm, and (C) bubble deformation occurring during electrospinning at 24 kV of applied voltage and 8 cm collection distance using 7 wt % PVA and 0.1 wt % Rhodamine B dye for visualization. [Color figure can be viewed in the online issue, which is available at wileyonlinelibrary.com.]

distance (defined as the distance between the top of the funnel and the collector for comparison) on the yield and morphology of nanofibers produced in foam electrospinning were investigated using electric field strengths between 250 and 420 kV/m and collection distances of 6–10 cm. No fibers are produced below 250 kV/m, indicating a threshold electric field strength. Electric field strengths between 250 and 330 kV/m with collection distances of 6 and 8 cm yield sparse, nonuniform mats with signs of fiber fusion and other artifacts related to incomplete drying (films with fiber shaped outlines). Further, extensive fiber fusion can be seen directly above the funnel, likely caused by bubbles bursting and

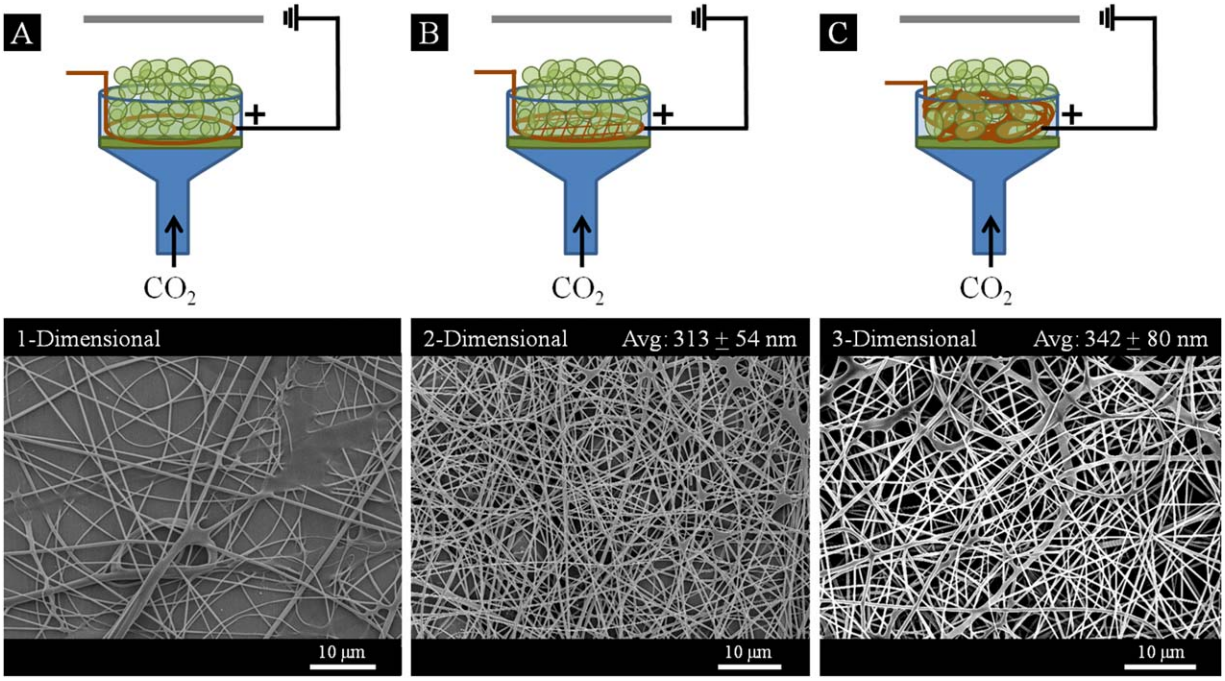

Figure 2. Schematics and resulting electrospun fibers for 7 wt % PVA in water utilizing (A) 1-D, (B) 2-D, and (C) 3-D electrodes.

[Color figure can be viewed in the online issue, which is available at wileyonlinelibrary.com.]

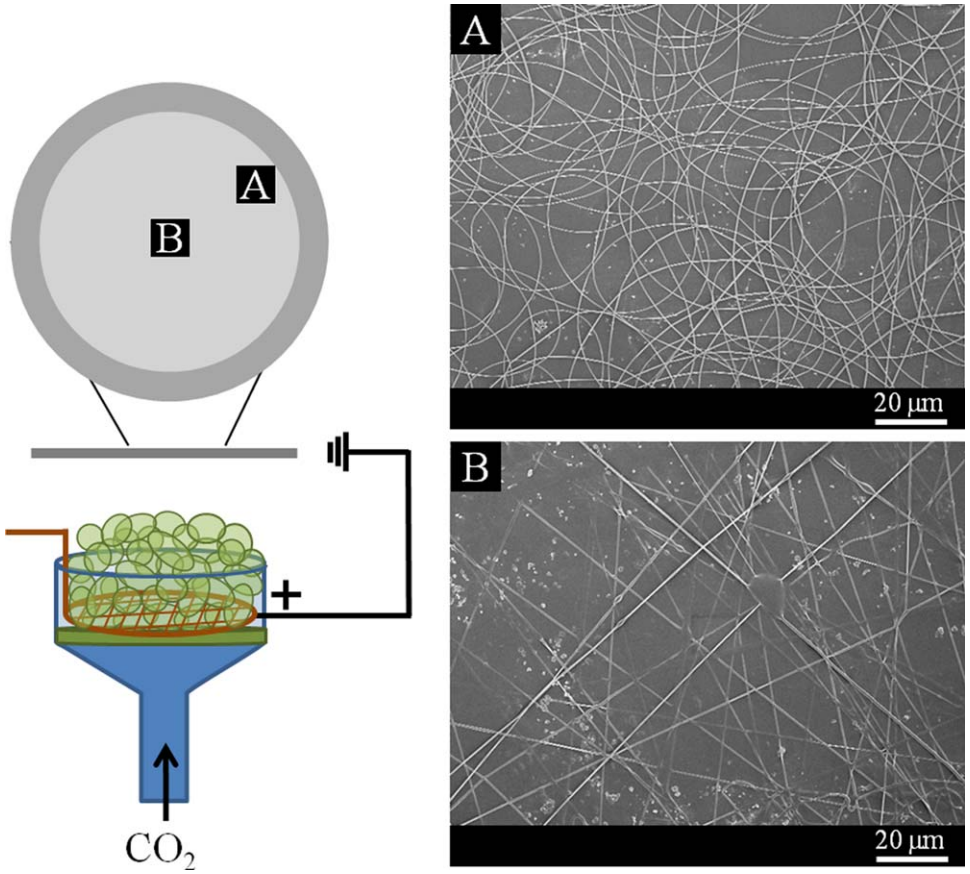

Figure 3. Foam electrospinning schematic and SEM micrographs showing the contrast in fiber morphology collected at a location (A) outside of the funnel and (B) directly above the fritted funnel at shortened collection distances.

[Color figure can be viewed in the online issue, which is available at wileyonlinelibrary.com.]

spreading solvent onto the surface of the collection plate, Figure 3B. Yet, a fibrous mat, Figure 3A, collects along the outer perimeter of the collection plate, which is located farther from the axis of the foamed column. However, increasing the collection distance to 10 cm provides ample time for solvent evaporation which minimizes solvent splatter and leads to smooth fiber morphology and mat uniformity (for additional micrographs, see Supporting Information).

Electric field strengths of 420 kV/m (the highest strength tested), yielded electrospun mats with excessive fiber fusion, despite changes in collection distance. At these electric fields, we observed entire bubbles being drawn out of the foam toward the collection plate, resulting in excessive solvent on the nonwoven mat (for additional micrographs, see Supporting Information). These results are comparable with electric field strengths previously reported for bubble spinning polyvinylpyrrolidone (PVP). However, fiber fusion was not reported when using PVP in a mixture of alcohol and water, likely due to the difference in solvent volatility.[25] Based on these results, there is an electric field strength window for the fabrication of uniform fibers via foam electrospinning, which is not generally observed in other methods of electrospinning, such as syringe electrospinning.

We note that during the electrospinning process, the foam protrudes approximately 1–2 cm above the funnel and are effectively the same for all experiments. Consequently, the actual distance between sample and collector is lower than the collection distance specified. This is analogous to the scenario in the fabrication of 3-D nanofiber web, which protrudes as a cotton candy like mesh from the collector plate.[32] Hence, the collection distance specified serves as a basis to quantify relative distances.

Concentration effects

In syringe electrospinning, it is generally accepted that polymer entanglement, predicted using solution dynamics, is required for the formation of fibers.[33–36] Empirically, the onset of beaded fibers occurs at the critical entanglement concentration (C_e), 2.5 wt % for aqueous PVA, indicated rheologically by a change in slope when plotting specific viscosity as a function of polymer concentration. The onset of uniform fibers, the critical concentration (C_c), generally occurs at 2–2.5 times C_e, that is, 6 wt % PVA,[31] Figure 4. Foam electrospinning concentrations below 2.5 wt % PVA result in dried polymer droplets due to deposition of debris from bursting bubbles and inadequate polymer entanglement, Figure 4, while 5 wt % PVA yields beaded fibers. Concentrations above 6 wt % PVA produce uniform fibers for both electrospinning methods, with fiber size increasing with concentration as expected (for additional micrographs and histograms of other concentrations, see Supporting Information).[37,38] Fiber distributions and average fiber diameters of 313 and 267 nm for 7 wt % PVA are comparable for foam electrospinning when compared to syringe electrospinning, respectively. Data shows the empirical guideline relating polymer entanglement and

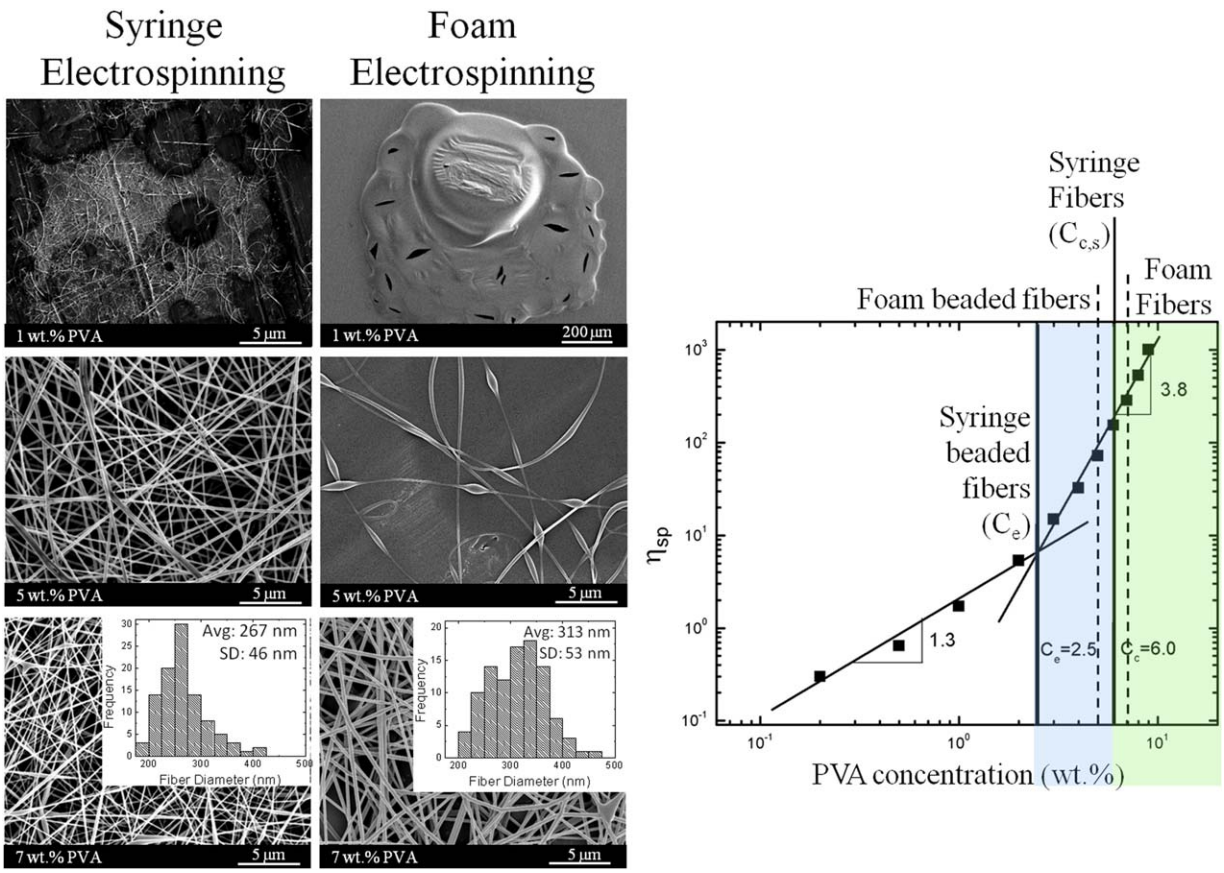

Figure 4. SEM micrographs comparing fibers fabricated from syringe and foam electrospinning using 1, 5, and 7 wt % PVA in water, with average fiber diameter and distribution for 7 wt % PVA.

Utilizing foam electrospinning, the concentration at which the onset of beaded and uniform fibers ($C_{c,f}$) is comparable to that required for syringe electrospinning, denoted as C_e and $C_{c,s}$, respectively, adapted.[31] ***The average fiber diameters and fiber distribution remain comparable for both electrospinning methods. [Color figure can be viewed in the online issue, which is available at wileyonlinelibrary.com.]

electrospun fiber morphology applies to foam electrospinning aqueous PVA solutions.

To demonstrate versatility, fibers from aqueous PEO were fabricated via foam electrospinning. Due to an increase in viscosity compared to PVA solutions, the coarse fritted funnel was used for electrospinning PEO solutions as the increased pore size facilitated foaming. Utilizing the previous empirical correlation, the critical entanglement concentration (C_e) of aqueous PEO occurs at 1.4 wt %, while the onset of uniform fibers, C_c, occurs at approximately 3.5 wt % PEO, Figure 5. Concentrations below 2 wt % result in polymer droplets, while 2 wt % produces beaded fibers for both electrospinning methods. Increasing the polymer concentration above 5 wt % PEO results in the fabrication of uniform nanofibers from both electrospinning methods, (for additional micrographs and histograms of higher concentrations, see Supporting Information). Further analysis for 5 wt % PEO shows that average fiber diameter and fiber distribution are comparable for both methods, Figure 6. We have shown the polymer concentrations required for fabrication of uniform electrospun fibers for PVA and PEO are comparable in foam and syringe electrospinning, further demonstrating that the relationship between polymer chain entanglement and uniform fiber fabrication also applies to the foam electrospinning process. Therefore, this relationship can serve as a guide to predict the electrospinnability of polymer solutions via foam electrospinning, implying that polymer systems found to electrospin uniform fibers via syringe electrospinning should produce uniform fibers via foam electrospinning.

To enhance the stability of the polymer foams to further facilitate electrospinning, Triton X-100® was added in 0.01 and 0.1 to 5 wt % PEO solutions. Addition of the surfactant resulted in polymer foams with increased cell quantity and size, measured qualitatively, while also extending the lifetime of the foams. Fibers fabricated from Triton X-100® infused foams show uniform morphology. A comparison of as spun fibers fabricated from syringe and foam electrospinning, Figure 6, shows the average diameters and fiber distributions remain comparable for both solutions containing up to 0.1 wt % Triton X-100®. Additionally, the average diameter and distribution of foam electrospun fibers seem unaffected by the addition of surfactant for 5 wt % PEO. This suggests that the addition of nonionic surfactant in small amounts to electrospinnable solutions can improve foam creation, without sacrificing desired fiber morphology.

As multiple jets form simultaneously, foam electrospinning can improve production rates when compared to syringe electrospinning. Typical throughputs for syringe electrospinning from a single needle range on the order of 5 to 20 μL/min. Experiments with 5 wt % PEO and 0.1 wt % Triton X-100® (added for foam stabilization) yield production rates as high as 1.5 mL/min. When foam electrospinning from a 30-mm diameter funnel, experimental results show a 300-fold increase in production rate, when compared to typical throughputs via

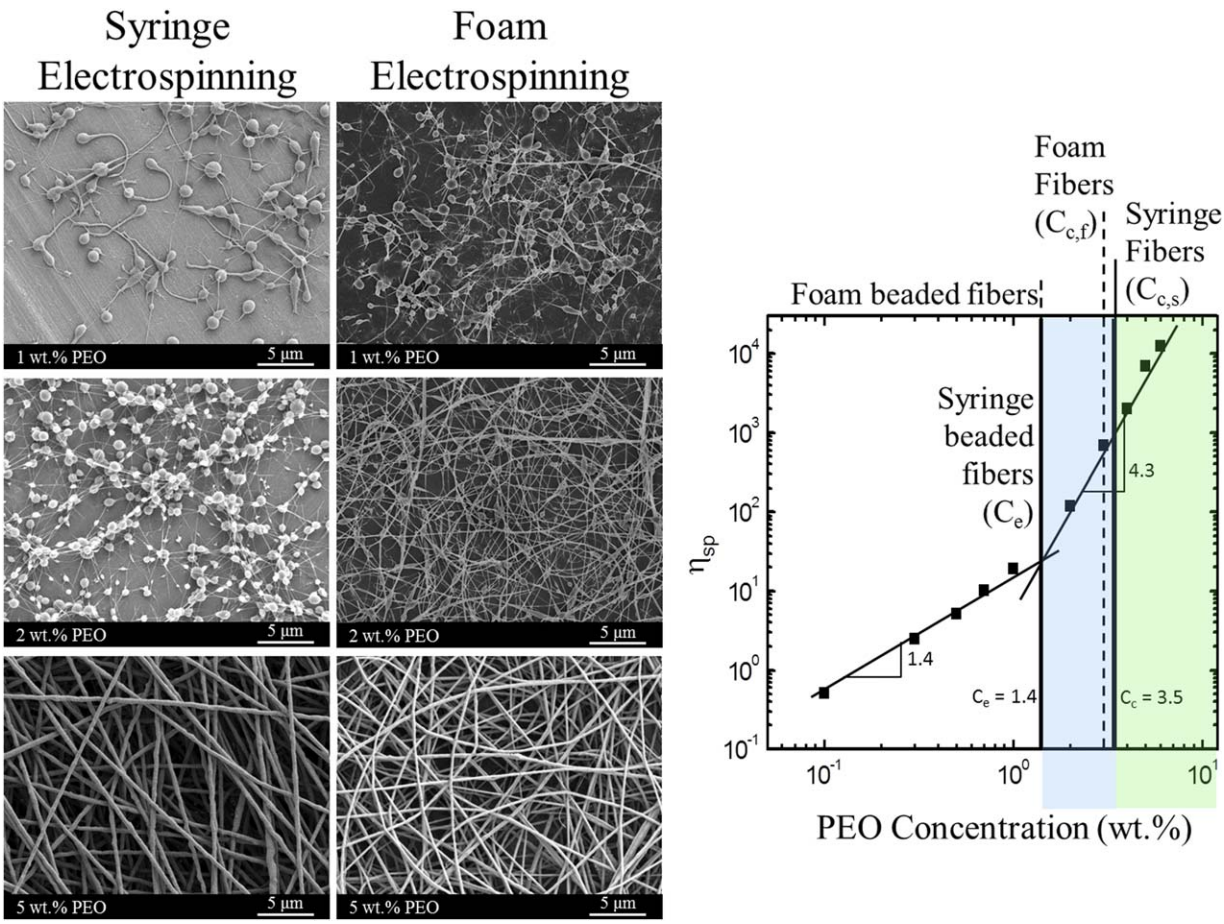

Figure 5. SEM micrographs comparing fibers fabricated from syringe and foam electrospinning using 1, 2, and 5 wt % PEO in water.

Utilizing foam electrospinning, the concentration at which beaded and uniform fibers ($C_{c,f}$) form is comparable to that required for syringe electrospinning, denoted as C_e and $C_{c,s}$, respectively. [Color figure can be viewed in the online issue, which is available at wileyonlinelibrary.com.]

syringe electrospinning. Whereas this assumes that all material from the funnel is converted to nanofibers, even if one assumes a substantial loss (e.g., 30%) in this regard due to bubble bursting and solvent evaporation, there is still more than two orders of magnitude increase in productivity. We believe increasing the size of the funnel and available surface area for foam electrospinning could further improve the production rate.

The Nanospider™ by Elmarco is widely used for high throughput production of electrospun nanofibers. For comparison, solutions of 7 and 9 wt % PVA were electrospun on the Nanospider™ using a droplet electrode accessory 10 mm in diameter, at varying voltages. SEM micrographs, Figure 7, show as spun fibers from the Nanospider™ but the defects in the nonwoven mat due to excessive solvent are evident. Figure 7 also shows SEM micrographs of uniform electrospun fibers fabricated from 7 and 9 wt % PVA solutions via syringe and foam electrospinning from a 30-mm diameter funnel. Although still in development, foam electrospinning provides an alternate approach for high throughput production of uniform electrospun nanofibers.

Electrospun fiber crystallinity

An interesting issue is the effect of electrospinning method on the crystallinity within resultant fibers. While studies report increase in crystallinity with electropinning, there is no report of the crystallinity of electrospun fibers from a curved surface as in foam electrospinning compared to the crystallinity of electrospun fibers from a bulk liquid as in syringe electrospinning. XRD measurements showing intensity as a function of 2θ for electrospun PEO fibers and as received PEO powder, Figure 8, show peaks at $2\theta = 19$ and 23°, which correspond to the 120 and 112 crystal planes, respectively.[39] The peak intensity decreases dramatically within electrospun fibers compared to the as received powder, independent of electrospinning method. This trend has been previously shown for various electrospinning systems.[39–42] In addition, higher-order reflections are seen for the as received powder at $2\theta = 26$–28°, which are indicative of well-developed crystalline microstructures. XRD measurements for foam electrospun samples of PEO and varying amounts of Triton X-100® show no significant change, further indicating the addition of surfactant does not change the fiber morphology or structure.

The percent crystallinity was quantified using DSC, endotherms shown in Figure 9, and calculated by normalizing the area under the curve with the heat of fusion for 100% crystalline PEO, reported as 197 J/g.[43,44] The percent crystallinity of 5 wt % PEO with and without surfactant for both foam and syringe electrospinning can be found in Table 1. As crystallinity within the electrospun fibers is due solely to the PEO content, percent crystallinity calculations for samples of PEO, and

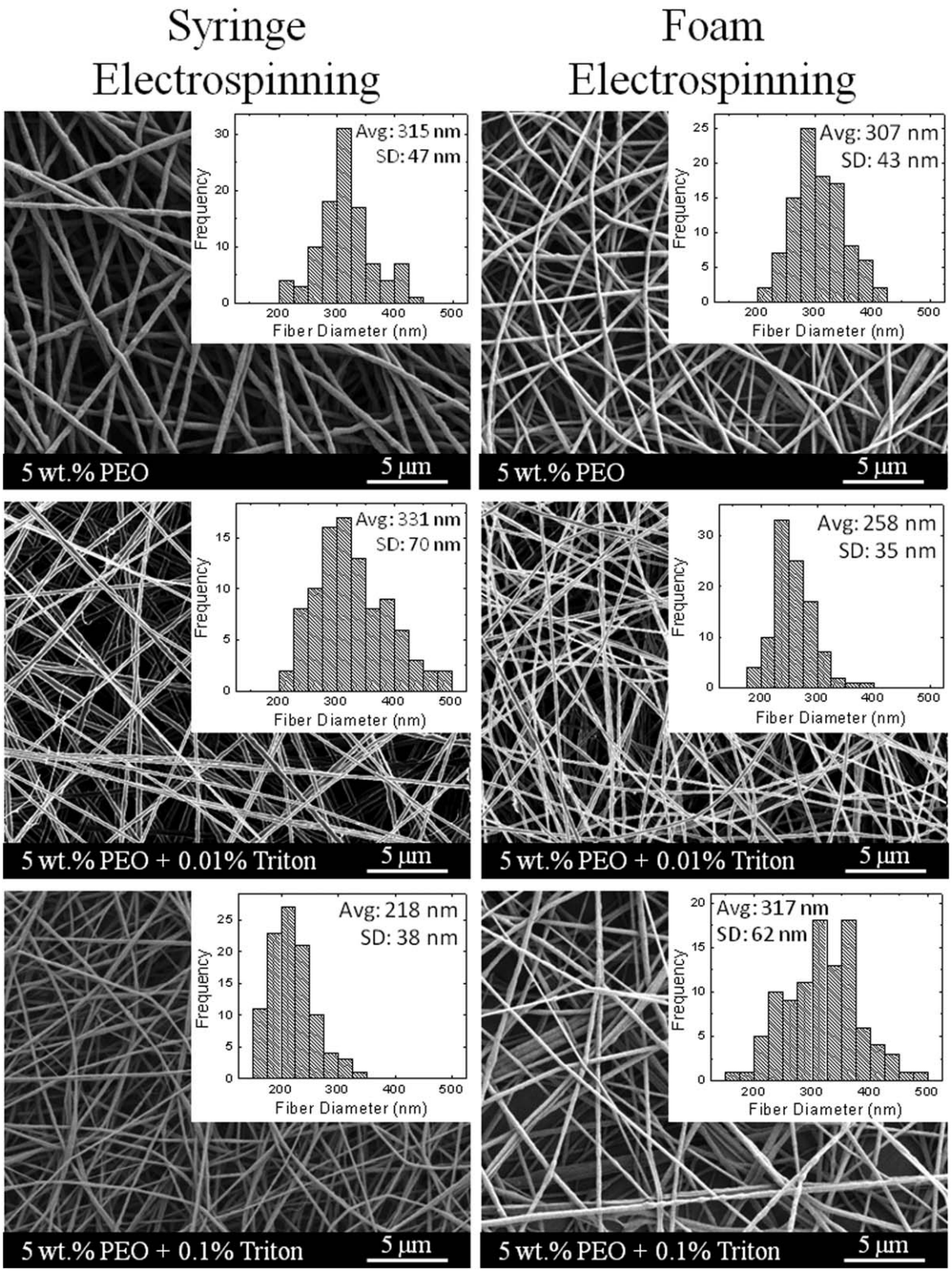

Figure 6. SEM micrographs and histograms comparing fibers fabricated from syringe and foam electrospinning using 5 wt % PEO, 5 wt % PEO with 0.01 wt % and 0.1 wt % Triton X-100® in water.

The fiber morphology, average diameter, and diameter distribution of electrospun fibers from foam electrospinning are comparable to syringe electrospinning.

surfactant were normalized by the weight proportion of PEO within the fibers. Crystallinity and the melting peak temperature of fibers produced via foam and syringe electrospinning methods is consistently lower than that of the PEO powder, corroborating data shown via XRD. It is believed that rapid solvent evaporation during processing hinders polymer chain interaction and thus crystallization within the polymer fiber.

Importantly, the percent crystallinity is consistently higher in fibers fabricated from foam electrospinning compared to syringe electrospun fibers, increasing from 70.3 to 78.5% for

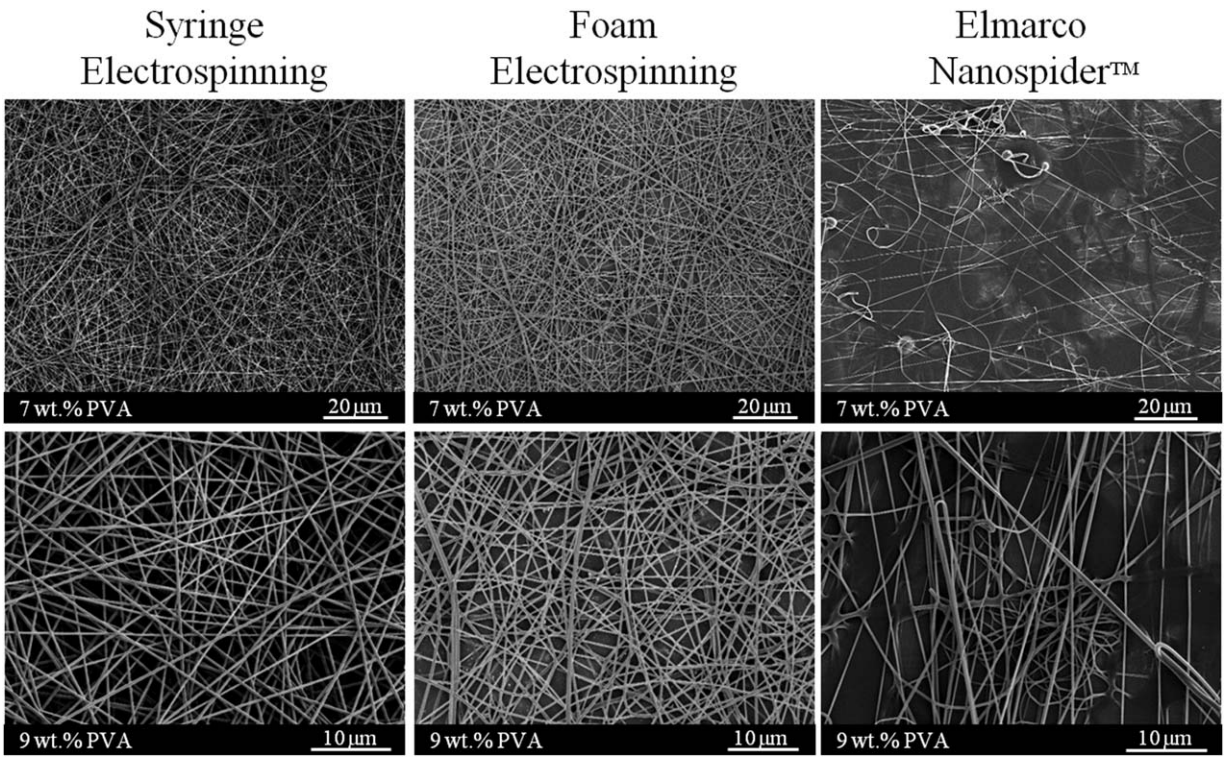

Figure 7. SEM micrographs of 7 and 9 wt % PVA fabricated via syringe electrospinning, foam electrospinning and the Nanospider™ by Elmarco.

Uniform fibers can be fabricated via syringe and foam electrospinning with higher mat quality compared to the Nanospider™ using a droplet electrode.

5 wt % PEO, and 67.5 to 75.1% when introducing 0.1 wt % Triton X-100®, shown in Table 1. Enhanced polymer crystallinity, even in modest amount, can lead to significant increase in fiber mechanical and structural properties such as tensile stength, yield stress, modulus,[45,46] and to degradation rates[47] and hydrophobicity[48] for tissue engineering applications. An improvement in crystallinity may be due to a combination of solvent evaporation and restricted chain orientation. As the foam electrospinning process is an open system, slow solvent evaporation and solvent drainage within the foam may occur over the duration of the experiment, increasing the effective concentration on the surface of the foam compared to the bulk concentration. It has been previously shown that concentration gradients within foams exist as the solvent gravitates toward points, where three or more cells meet (plateau border) for entropic reasons. Another contributing factor may be due to the restriction of chain orientation within the thin bubble surface, possibly promoting

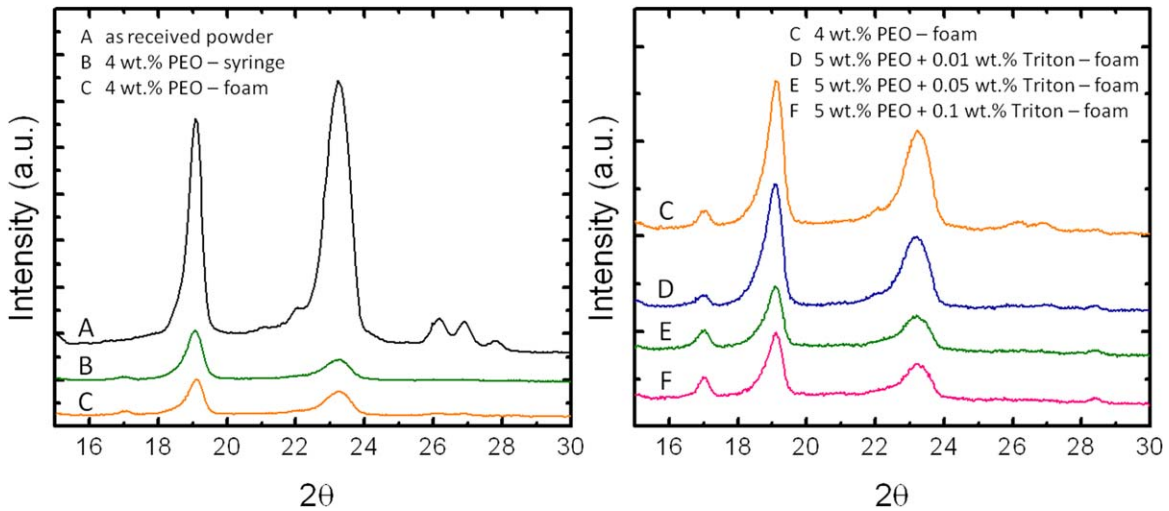

Figure 8. Plots of the intensity as a function of 2θ from XRD measurements comparing electrospun fibers from syringe and foam electrospinning with as received PEO powder.

Additional XRD measurements of fibers created via foam electrospinning with varying amounts of Triton X-100®. [Color figure can be viewed in the online issue, which is available at wileyonlinelibrary.com.]

biaxial orientation of the polymer chains. As the chance for polymer chain interactions increases, polymer crystal formation and growth is promoted. These factors will need to be investigated in future articles.

Results from this work lay the initial foundation for foam electrospinning as a methodology to build upon. Similarity in fiber size and morphology between syringe and foam electrospinning seem to indicate that the intricate details of foam dynamics may not be a critical factor in this electrospinning process. Nevertheless, the foam produced in this study were polydisperse, and it would be useful to control the bubble size and develop foams with controlled but different bubble sizes and see how that affects electrospinning, in particular the production. This would lead us to examine if bubble size affects electrospinnability and fiber production rate. Another parameter of interest would be to produce foam of different gas volume fraction. If indeed film properties dictate crystallinity, we should be able to control it by varying foam lamellae thickness using foam of different quality. In its ideal state, one can envision development of a continuous process in which liquid and gas are fed at a specified rate to maintain foam production commensurate with that of fiber production. Many such intriguing issues present themselves, and can form the subject of future endeavors.

Conclusions

We demonstrate a multiple jet electrospinning technique wherein nanofibers are produced from foamed polymer solutions. Distribution of electrical charge throughout the bulk of the foam is necessary for the formation of uniform fibers. An electric field strength window exists for the formation of uniform fibers via foam electrospinning. When the electric field strength is too weak, little to no fibers form, while stronger fields result in a fiber-infused film. At a given electric field strength within the electrospinning window, increased collection distances aid in sufficient solvent evaporation, improving mat uniformity. Concentrations at which beaded and uniform fibers form using foam electrospinning and the resulting fiber sizes are comparable to those reported in syringe electrospinning for PVA and PEO for all concentrations presented. This work shows that the relationship between polymer entanglement and fiber formation in electrospinning holds for this process. The addition of surfactant in the case of PEO improves production rate while fiber diameter and distribution remain unaffected. Production rates for foam electrospinning were improved as much as 300 times compared to syringe electrospinning. Fiber crystallinity was also enhanced via foam electrospinning, most likely due to the combination of gradual solvent evaporation, biaxial polymer chain orientation within the thin film bubble boundary, and increased effective concentration on the foam surface, promoting chain interactions and polymer crystal formation and growth. Foam electrospinning serves as an alternate approach to nanofiber fabrication with improved production rate and fiber crystallinity, without the need for alterations or additional experiments to discover appropriate conditions, as the parameters and trends for uniform fiber fabrication are comparable to syringe electrospinning.

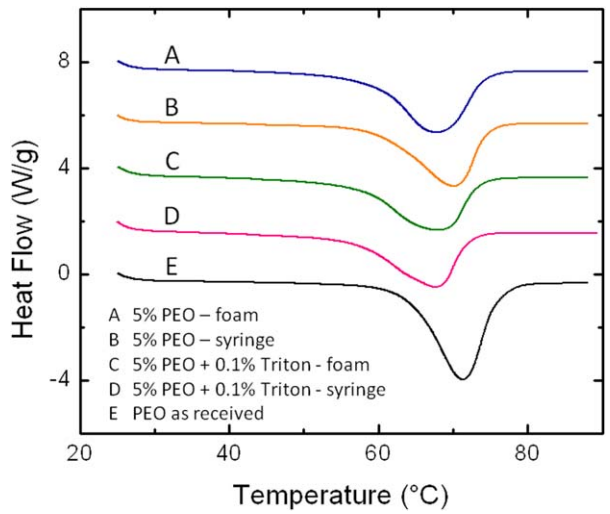

Figure 9. DSC melting endotherms of electrospun fibers utilizing foam electrospinning and syringe electrospinning from various PEO solutions along with as received PEO powder.

[Color figure can be viewed in the online issue, which is available at wileyonlinelibrary.com.]

Table 1. Percent Crystallinity and Melt Peak Temperatures as Measured by DSC of Various PEO Solutions Using Foam Electrospinning and Syringe Electrospinning

System	Electrospinning Method	Melt Peak Temperature (°C)	% Crystallinity
PEO as received	–	71.1	92.5 ± 0.1
5% PEO	Foam	67.5	78.5 ± 0.1
	Syringe	70.1	70.3 ± 0.1
5% PEO + 0.1% Triton X-100®	Foam	67.7	75.1 ± 0.1
	Syringe	68.5	72.5 ± 0.1

Acknowledgments

This work was supported in part by The Nonwovens Cooperative Research Center (NCRC) and a Graduate Assistance in Areas of National Need (GAANN) fellowship through the Dept of Education. The authors would like to thank Dr. Ralph Colby, Dr. Robert Prud'homme, Dr. Jan Genzer, and Dr. Maury Balik for their input on polymer orientation and crystallization, Dr. Joshua Manasco for his help in discussion and construction of the apparatus, and Dr. Sara Arvidson and Nancy Burns for their discussions and assistance with the research presented here.

Literature Cited

1. Katti DS, Robinson KW, Ko FK, Laurencin CT. Bioresorbable nanofiber-based systems for wound healing and drug delivery: optimization of fabrication parameters. *J Biomed Mater Res B Appl Biomater*. 2004;70:286–296.
2. Formo E, Lee E, Campbell D, Xia Y. Functionalization of electrospun TiO2 nanofibers with Pt nanoparticles and nanowires for catalytic applications. *Nano Lett*. 2008;8:668–672.
3. Kim GH, Yoon H. A direct-electrospinning process by combined electric field and air-blowing system for nanofibrous wound-dressings. *Appl Phys A*. 2008;90:389–394.
4. Kim K, Luu YK, Chang C, Fang DF, Hsiao BS, Chu B, Hadjiargyrou M. Incorporation and controlled release of a hydrophilic antibiotic using poly(lactide-co-glycolide)-based electrospun nanofibrous scaffolds. *J Controlled Release*. 2004;98:47–56.
5. Li D, McCann JT, Xia YN. Use of electrospinning to directly fabricate hollow nanofibers with functionalized inner and outer surfaces. *Small*. 2005;1:83–86.
6. Liao Y, Zhang L, Gao Y, Zhu Z, Fong H. Preparation, characterization, and encapsulation/release studies of a composite nanofiber mat

electrospun from an emulsion containing poly(lactic-co-glycolic acid). *Polymer (Guildf)*. 2008;49:5294–5299.
7. Schreuder-Gibson H, Gibson P, Senecal K, Sennett M, Walker J, Yeomans W, Ziegler D, Tsai PP. Protective textile materials based on electrospun nanofibers. *J Adv Mater*. 2002;34:44–55.
8. Li D, Babel A, Jenekhe SA, Xia YN. Nanofibers of conjugated polymers prepared by electrospinning with a two-capillary spinneret. *Adv Mater*. 2004;16:2062–2066.
9. Reneker DH, Chun I. Nanometre diameter fibres of polymer, produced by electrospinning. *Nanotechnology* 1996;7:216–223.
10. Reneker DH, Yarin AL, Fong H, Koombhongse S. Bending instability of electrically charged liquid jets of polymer solutions in electrospinning. *J Appl Phys*. 2000;87:4531–4547.
11. Huang ZM, Zhang YZ, Kotaki M, Ramakrishna S. A review on polymer nanofibers by electrospinning and their applications in nanocomposites. *Compos Sci Technol*. 2003;63:2223–2253.
12. Taylor G. Disintegration of water drops in electric field. *Proc R Soc London Ser A*. 1964;280:383–397.
13. Hohman MM, Shin M, Rutledge G, Brenner MP. Electrospinning and electrically forced jets. II. Applications. *Phys Fluids*. 2001;13: 2221–2236.
14. Hohman MM, Shin M, Rutledge G, Brenner MP. Electrospinning and electrically forced jets. I. Stability theory. *Phys Fluids*. 2001;13: 2201–2220.
15. Dosunmu OO, Chase GG, Kataphinan W, Reneker DH. Electrospinning of polymer nanofibres from multiple jets on a porous tubular surface. *Nanotechnology* 2006;17:1123–1127.
16. Niu H, Lin T, Wang X. Needleless electrospinning. I. A comparison of cylinder and disk nozzles. *J Appl Polym Sci*. 2009;114:3524–3530.
17. Theron SA, Yarin AL, Zussman E, Kroll E. Multiple jets in electrospinning: experiment and modeling. *Polymer* 2005;46:2889–2899.
18. Wang D, Sun G, Chiou B, Hinestroza JP. Controllable fabrication and properties of polypropylene nanofibers. *Polym Eng Sci*. 2007;47: 1865–1872.
19. Wang X, Niu H, Lin T, Wang X. Needleless electrospinning of nanofibers with a conical wire coil. *Polym Eng Sci*. 2009;49:1582–1586.
20. Yarin AL, Zussman E. Upward needleless electrospinning of multiple nanofibers. *Polymer*. 2004;45:2977–2980.
21. Liu Y, He J. Bubble electrospinning for mass production of nanofibers. *Int J Nonlinear Sci Numer Simul*. 2007;8:393–396.
22. Liu Y, He J, Xu L, Yu J. The principle of bubble electrospinning and its experimental verification. *J Polym Eng*. 2008;28:55–65.
23. Liu Y, Ren Z-F, He J-H. Bubble electrospinning method for preparation of aligned nanofibre mat. *Mater Sci Technol*. 2010;26:1309–1312.
24. He J, Liu Y, Xu L, Yu J, Sun G. BioMimic fabrication of electrospun nanofibers with high-throughput. *Chaos Solitons Fractals*. 2008;37:643–651.
25. Liu Y, Dong L, Fan J, Wang R, Yu J. Effect of applied voltage on diameter and morphology of ultrafine fibers in bubble electrospinning. *J Appl Polym Sci*. 2011;120:592–598.
26. Ren Z, He J. Single polymeric bubble for the preparation of multiple micro/nano fibers. *J Appl Polym Sci*. 2011;119:1161–1165.
27. Yang R, He J, Yu J, Xu L. Bubble-electrospinning for fabrication of nanofibers with diameter of about 20nm. *Int J Nonlinear Sci Numer Simul*. 2010;11:163–164.
28. Yang R-R, He J-H, Xu L, Yu J-Y. Effect of solution concentration on diameter and morphology of PVA nanofibres in bubble electrospinning process. *Mater Sci Technol*. 2010;26:1313–1316.
29. Varabhas JS, Tripatanasuwan S, Chase GG, Reneker DH. Electrospun jets launched from polymeric bubbles. *J Eng Fiber Fabr*. 2009; 4:46–50.
30. Teo WE, Ramakrishna S. A review on electrospinning design and nanofibre assemblies. *Nanotechnology*. 2006;17:R89–R106.
31. Tang C, Saquing CD, Harding JR, Khan SA. In situ cross-linking of electrospun poly(vinyl alcohol) nanofibers. *Macromolecules*. 2010; 43:630–637.
32. Bonino CA, Efimenko K, Jeong SI, Krebs MD, Alsberg E, Khan SA. Three-dimensional electrospun alginate nanofiber mats via tailored charge repulsions. *Small*. 2012;8:1928–1936.
33. Koski A, Yim K, Shivkumar S. Effect of molecular weight on fibrous PVA produced by electrospinning. *Mater Lett*. 2004;58:493–497.
34. McKee MG, Wilkes GL, Colby RH, Long TE. Correlations of solution rheology with electrospun fiber formation of linear and branched polyesters. *Macromolecules*. 2004;37:1760–1767.
35. Shenoy SL, Bates WD, Wnek G. Correlations between electrospinnability and physical gelation. *Polymer*. 2005;46:8990–9004.
36. Shenoy SL, Bates WD, Frisch HL, Wnek GE. Role of chain entanglements on fiber formation during electrospinning of polymer solutions: good solvent, non-specific polymer-polymer interaction limit. *Polymer*. 2005;46:3372–3384.
37. Gupta P, Elkins C, Long TE, Wilkes GL. Electrospinning of linear homopolymers of poly(methyl methacrylate): exploring relationships between fiber formation, viscosity, molecular weight and concentration in a good solvent. *Polymer*. 2005;46:4799–4810.
38. Deitzel JM, Kleinmeyer J, Harris D, Tan NCB. The effect of processing variables on the morphology of electrospun nanofibers and textiles. *Polymer*. 2001;42:261–272.
39. Deitzel JM, Kleinmeyer JD, Hirvonen JK, Tan NCB. Controlled deposition of electrospun poly(ethylene oxide) fibers. *Polymer*. 2001;42: 8163–8170.
40. Inai R, Kotaki M, Ramakrishna S. Structure and properties of electrospun PLLA single nanofibres. *Nanotechnology*. 2005;16:208–213.
41. Li CM, Vepari C, Jin HJ, Kim HJ, Kaplan DL. Electrospun silk-BMP-2 scaffolds for bone tissue engineering. *Biomaterials*. 2006;27: 3115–3124.
42. Zhang D, Karki AB, Rutman D, Young DR, Wang A, Cocke D, Ho TH, Guo Z. Electrospun polyacrylonitrile nanocomposite fibers reinforced with Fe3O4 nanoparticles: fabrication and property analysis. *Polymer*. 2009;50:4189–4198.
43. Wunderlich B. Thermal Analysis. San Diego, CA: Academic Press, 1990.
44. Talwar S, Krishnan AS, Hinestroza JP, Pourdeyhimi B, Khan SA. Electrospun nanofibers with associative polymer-surfactant systems. *Macromolecules*. 2010;43:7650–7656.
45. Ero-Phillips O, Jenkins M, Stamboulis A. Tailoring crystallinity of electrospun plla fibres by control of electrospinning parameters. *Polymers*. 2012;4:1331–1348.
46. Lewin M. (ed). Handboof of Fiber Chemistry. 3rd ed. CRC Press (Boca Raton FL); 2010.
47. Middleton J, Tipton A. Synthetic biodegradable polymers as orthopedic devices. *Biomaterials*. 2000;21:2335–2346.
48. Areias AC, Ribeiro C, Sencadas V, et al. Influence of crystallinity and fiber orientation on hydrophobicity and biological response of poly(L-lactide) electrospun mats. *Soft Matter*. 2012;8:5818–5825.

Manuscript received Nov. 25, 2013, and revision received Jan. 6, 2014.